

Can gas phase calculations be effective in generating the novel chemistry of organic-inorganic halide perovskite solar cells?

(Department of Chemical System Engineering, School of Engineering, The University of Tokyo, 7-3-1 Hongo, Bunkyo-ku, Japan 113-8656)

○ Pradeep R. Varadwaj, Arpita Varadwaj, Koichi Yamashita

E-mail: pradeep@tcl.t.u-tokyo.ac.jp

[Introduction] The organic-inorganic methylammonium lead(tin/germanium) halide hybrid perovskites, symbolically $\text{MAPb}(\text{Sn}/\text{Ge})\text{X}_3$ ($\text{X} = \text{Cl}, \text{Br}, \text{I}$), are a specific class of mineral based novel photocatalytic systems. They are magically so feverish and so natural that they have gone viral in solar sector today to advance scientific research in future energy technology.¹ An underlying reason for which they are considered as most crucial lies in their technological adamant in the solar technology race since they can take the sunlight in and generate the electricity out similar to any novel photo-catalyst.^{2,3} The perovskites fall in the class of low band gap materials such that their band gap in the 1.5–3.1 eV can be tunable changing the halogen and metal contents.² Another reason for which scientists put too much emphasis on these lies in their unique chemico-physical, electrical, optoelectronic, and materials properties that are least understood, needing further exploration covering areas as diverse as, *inter alia*, chemistry, physics, electrical, electronic synthetic and chemical engineering, crystallography, and in materials science and nanotechnologies.³ The importance of these highly-valued materials can be realized by surveying the Web of science database. For instance, searching the simple keyword “lead halide perovskite” displays about 1200 peer reviewed publications catalogued in the literature. Our survey is consistent with Manser et al.^{4a)} who have claimed a dramatic rise in the number of PSC-related publications to be more than 1100 from just a single primary article appeared in 2009 (the first one?), which are accompanied with 28000 indexed citations in 2015.

Researchers classify the $\text{MAPb}(\text{Sn}/\text{Ge})\text{X}_3$ perovskites as third-generation photovoltaic solar cell materials.⁵ Their extraordinary device-based photon conversion performances gleaned within last five years have recently enforced Stoumpos et al. to refer these materials, as well as some of their mixed halogen derivatives $\text{CH}_3\text{NH}_3\text{Pb}(\text{Sn}/\text{Ge})(\text{X}_y\text{I}_{3-y})_{z=0-3}$ ($\text{X} = \text{Cl}, \text{Br}$), to as a class of the poor man’s high performance semiconductors.^{6a)} even though they are not set ready for outdoor activities. An important reason for which these systems are put at the first place lies in their elemental constituents that are abundant, and cost-effective. They are also technologically advantageous over other known solar cells, e.g., silicon solar cells, GaAs, and CdSe, and organic solar cells, etc. These materials are easy-to-synthesize even in traditional/ordinary research laboratories, and are easily processable in solution. Because of these latter features they are competitive with the dye-sensitized solar cells, as well as with organic photovoltaic solar cells, in terms of device fabrication, and processing, etc.⁴

Sum and Park have realized that despite the expeditious research progress on halide perovskite solar cells, a comprehensible understanding of their fundamental and device-based sciences, e.g. interfacial charge dynamics, and origins of the current-voltage hysteresis, etc., is still lacking.^{6b)} Therefore, attentive involvements of interdisciplinary groups of researchers with diverse scientific backgrounds are needed to address the nontrivial issues.

We are basically interested in part in the enhancement of the current understanding of the coordination and noncovalent chemistry, the origins of ferroelectricity, and the environmental instabilities, etc., of the halide perovskite materials. This is so as unambiguous and profound knowledges on these fundamental themes are essentially important in the strategic and controllable designs of novel materials of such kind.

In this presentation, we focus to discuss the density functional theory gas phase results of the structural, energetic, one-electron, charge density topological, and molecular orbital features (i) of the neutral clusters of lead trihalide anion (PbX_3^-) with methylammonium organic cation (CH_3NH_3^+), (ii) of the cationic and neutral clusters of the PbX_6^{4-} octahedral species with the organic cation, in which, each face of the octahedron occupies with one unit of the organic cation upon successive addition (same as in Fig. 1), and (iii) of the cationic clusters of $[(\text{CH}_3\text{NH}_3)_3\text{PbX}_6]^{4+}$ with water (H_2O) molecule(s). For the latter case, the number of H_2O molecules range from one up to ten. The coordination and physical chemistry of the above-mentioned clusters, especially the latter ones, are expected to have strong relevance with those of the $[(\text{CH}_3\text{NH}_3)_4\text{Pb}_6(\text{H}_2\text{O})_{n=1,2}]$ zero-dimensional (0D) quantum dot structures. The targeted results of this investigation concern (i) the identification of various coordination/dative and noncovalent interactions in the halide perovskites and their subsequent characterizations, (ii) the estimations of the natures and strengths of such interactions and their importances in the rationale designs, (iii) the prediction and elucidation of the structural accuracies and energetic stabilities of the perovskite species in aqueous environments, and their relation with the corresponding gas phase properties, and, (iv) the exploration of whether or not the chemical physics of the small model clusters examined can adequately assist in understanding the large scale 2D/3D images of the halide perovskites.

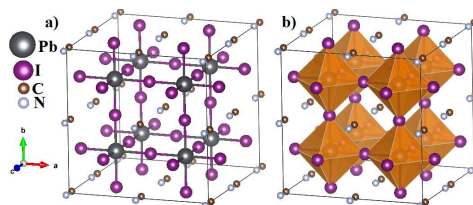


Fig. 1: The a) ball and stick, and b) polyhedral models of the pseudocubic phase of the MAPbI_3 perovskite, analogous with the one reported in the solid state (Cambridge Structural Database (CSD) ref. code MAPBTI02). Both displays the facial part of each PbI_6^{4-} octahedron is equipped with an MA cation. For clarity, the H atoms are not shown.

[Results and Discussions] In the $\text{MAPb}(\text{Sn}/\text{Ge})\text{X}_3$ ($\text{X} = \text{Cl}, \text{Br}, \text{I}$) perovskites in higher dimensions, regardless of their structural diversities (monoclinic, orthorhombic, tetragonal, or pseudocubic), the eight faces of the $[\text{PbX}_6]^{4-}$ corner sharing octahedron are perhaps equipped with eight organic cations. For clarity, the attribute is displayed in Fig. 1 for the pseudocubic phase of the MAPbI_3 perovskite (also see Fig. 1 of abstract 3E04 for monoclinic phase). In any circumstances, the organic cations play a role similar to that of spacers, or soft-glues, or clamps, which assist in holding the $[\text{PbX}_6]^{4-}$ octahedra together in layers in the 2D/3D perovskite films. In its simplest representation, no matter whether solid/gas, the geometrical structure of any $\text{MAPb}(\text{Sn}/\text{Ge})\text{X}_3$ perovskite is a combination of two species, the $[\text{Pb}(\text{Sn}/\text{Ge})\text{X}_3]^-$ inorganic core (a strong base), and the CH_3NH_3^+ organic surrounding (a strong acid). This can be realized from Fig. 2, illustrated for the $\text{CH}_3\text{NH}_3\text{PbI}_3$ cluster, for example. Clearly, the unified arrangement is the result of the marriage between an acid and a base comprising polarities of two kinds. This is of course driven by the donation of an appreciable

amount of electron densities ($\sim 0.2\text{--}0.3 e$) from the electron rich orbital of the anion to an empty orbital of the cation. A consequence of this is an emergence of an extensive network of hydrogen bonding interactions operated by electrostatics forces. Evidently, whatever the occasion is, the absence of the above-mentioned attractive interactions would not allow the halide perovskites to have any real physical existence.

While it is not possible here to discuss the detailed structural and energetic stability preferences between all kinds of the halide perovskites examined, we present only the results of the $\text{CH}_3\text{NH}_3\text{PbI}_3$ clusters. The M06-2X/ADZP and PBE/ADZP binding energies for the most stable $\text{CH}_3\text{NH}_3\text{PbI}_3$ cluster were computed to be -125.1 and -129.2 kcal mol $^{-1}$, respectively. The slight variation in the binding energy is not unexpected as the percentages of exchange and correlation mixing in the two DFT functionals are different. The binding energy can be tunable depending on the physical orientation of the MA species around the facial part of the PbI_3^- . Accordingly, such an orientation has led to the formation another three conformers whose energies nonetheless are not small, values lying between -95.1 and -129.2 kcal mol $^{-1}$ with PBE/ADZP, and that between -93.5 and -125.1 kcal mol $^{-1}$ with M06-2X/ADZP (see Fig. 2 for conformational details). Indeed these energies are orders of magnitude larger than the range of values known for noncovalent interactions, varying in strength from very weak (-0.2 and -0.5 kcal mol $^{-1}$) to extremely strong (e.g., -40.5 kcal mol $^{-1}$ for $\text{F}\cdots\text{H}\cdots\text{F}$). The result enables us to conclude that the $\text{I}\cdots\text{H}\cdots\text{N}$ and $\text{I}\cdots\text{H}\cdots\text{C}$ hydrogen bonding interactions emanated of the halide perovskites are *not just ordinary ionic interactions*, but are rare, specific, directional and contain significant amount of covalent character. Of course, electrostatics, induction, polarization, and dispersion interactions, etc., together with solvation, crystal packing forces, among others, are the key cornerstones collectively providing rigidity to the entire geometries of the perovskite films in the crystalline phase.

Fig. 3 illustrates the energy-minimized geometries of the $[\text{PbX}_6]^{2+}$ bare ion, and its multinary clusters with MA. Despite several attempts, the cluster of PbI_6^{4-} with a single MA species, as well as that with three MA species, could not be energy-minimized. While the first arrangement led to the dissociation of the PbI_6^{4-} octahedron (upon its interaction with the MA species), the latter arrangement involving the three MA species resulted in frequent convergence error. A similar failure was also noticed when the two MA subunits were asymmetrically placed around the PbI_6^{4-} core. However, with some effort the geometry optimization of the latter arrangement resulted in a clustered species comprising the tetrahedral PbI_4^{2-} and the $\text{I}\cdots\text{H}\cdots\text{CH}_3\text{NH}_3$ hydrogen bonded ion-pairs, Fig. 3b). The abnormal feature was not turned on when two MA species were placed symmetrically around the two faces of the PbI_6^{4-} core, with the computed binding energy of -558.8 kcal mol $^{-1}$ for the resulting cluster, see Fig. 3c). This result is analogous to an experimental observation of Leguy et al. who have found that the hydration process is isotropic and homogeneous throughout the perovskite film.^{7a)} Nevertheless, as might be realized from Fig. 3, the (stepwise) binding energy monotonically increases from -558.8 to -941.3 kcal mol $^{-1}$ by increasing up to six MA species around the PbI_6^{4-} ion. Adding more MA species (i.e., increasing the number of MA species from 6 through 7 to 8) around the PbI_6^{4-} ion has resulted in a decreasing tendency for the binding energy, with ΔE becoming -785.8 kcal mol $^{-1}$ for the $[\text{PbI}_6(\text{CH}_3\text{NH}_3)_8]^{4+}$ cluster (for full energetic details see Fig. 3), a consequence of steric crowding. Full structural, and charge transfer features for all the clusters will be discussed in detail during the course of the presentation.

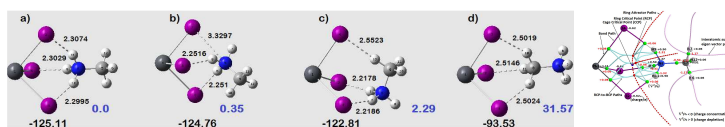


Fig. 2 The M06-2X/ADZP conformations of the $\text{CH}_3\text{NH}_3\text{PbI}_3$ binary cluster, a)–d). Shown are the relative energies (numbers in blue in kcal mol $^{-1}$), the binding energies (numbers in bold black in $\Delta E/\text{kcal mol}^{-1}$), and some selected intermolecular bond distances (numbers in bold black in Å) for the clusters. The graphic on the extreme right represents the QTAIM molecular graph for the most stable conformer a), obtained with the same level of theory. Among some properties, it illustrates the (3,-1) bond (ring and cage) critical points, the bond paths in atom colors connecting bonded atomic basin paths, and the basin gradient paths.

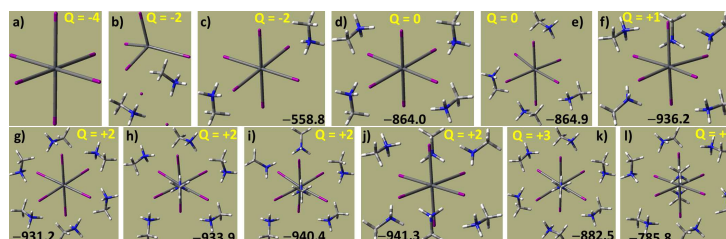


Fig. 3: PBE/DZP energy minimized geometries of the clusters of PbI_6^{4-} with MA. These include a) $[\text{PbX}_6]^{2+} (O_h)$, b) $(\text{CH}_3\text{NH}_3)_2^{2+} \cdot 2\Gamma^- [\text{PbX}_6]^{2-} (C_2)$, c) $(\text{CH}_3\text{NH}_3)_2^{2+} \cdot [\text{PbX}_6]^{2+} (C_2)$, d–e) $(\text{CH}_3\text{NH}_3)_4^{4+} \cdot [\text{PbX}_6]^{2+} (C_2, C)$, f) $(\text{CH}_3\text{NH}_3)_4^{4+} \cdot [\text{PbX}_6]^{2+} (C)$, g–j) $(\text{CH}_3\text{NH}_3)_6^{6+} \cdot [\text{PbX}_6]^{2+} (S_6, C_3, C_2, C)$, k) $(\text{CH}_3\text{NH}_3)_7^{7+} \cdot [\text{PbX}_6]^{2+} (C)$, and l) $(\text{CH}_3\text{NH}_3)_8^{8+} \cdot [\text{PbX}_6]^{2+} (C)$, where the terms in italics represent the point group symmetries. Shown are the net charges (Q/e) and the overall binding energies (kcal mol $^{-1}$) of latter ten cluster systems.

The HOMO-LUMO gaps in molecules, as well as in molecular clusters, represent the difference in energies between the highest occupied and the lowest unoccupied molecular orbitals. It has comparable significance with band gap generally referred in the solid state. For the latter, the gap represents the energy difference between the top of the valence band and the bottom of the conduction band. Benchmark calculations comprising 35 DFT functionals, together with the HF and MP2 methods, were performed to assess their dependences on the HOMO-LUMO gaps for the most and least stable $\text{CH}_3\text{NH}_3\text{PbI}_3$ clusters (see Fig. 1). Majority of the functionals incorporating 0–22 % Hatree-Fock exchange have predicted the energy gap in the 2.07 – 4.24 eV range for the clusters, comparable with the PBE/DZP estimates; all utilized the M06-2X/ADZP optimized geometries for the two clusters. The gap is a little affected for the $[(\text{CH}_3\text{NH}_3)_{n=0,2,4,8}\text{PbI}_6]^{2-4+}$ and $[(\text{CH}_3\text{NH}_3)_8\text{PbI}_6]^{4+} \cdot (\text{H}_2\text{O})_{n=1-10}$ octahedral clusters, all < 3.3 eV with PBE/DZP. The large optical gap for the (0D) quantum dot perovskite materials is not very astonishing as such gaps have strong dependence on the dimensionality, that is, it increases with the size of the perovskite material passing from 3D to 2D to 1D to 0D. All the results above suggest that the gas phase calculations do provide an additional dimension that enhances the current understanding of the novel physical chemistry of the organic-inorganic halide perovskite solar cell materials, probably consistent with others.^{7b)–c)}

[References]

- S. D. Stranks et al., Nat. Nanotech. 2015, 10, 391.
- The future of low-cost solar cells. M. Jacoby, C & EN news, 2016, 94, 30.
- a) M. M. Lee, Science 2012, 338, 643; b) T. -B. Song et al., J. Mater. Chem. A 2015, 3, 9032.
- a) J. S. Manser et al., Acc. Chem. Res. 2016, 49, 330; b) B. Saparov et al., Chem. Rev. 2016, 116, 4458; c) D. Li et al., J. Phys. Chem. C 2016, 120, 6363; d) J. M. Frost, Nano Lett. 2014, 14, 2584; e) T. A. Berhe et al., Energy Environ. Sci. 2016, 9, 323.
- J. Yan, B. R. Sounders, RSC Adv. 2014, 4, 43286; b) T. C. Sum et al., Acc. Chem. Res. 2016, 49, 294.
- a) C. C. Stoumpos, M. G. Kanatzidis, Adv. Mat. 2016, 28, 5778; b) For details see the editorial text “focus on perovskite solar cells” available at: <http://iopscience.iop.org/journal/0957-4484/page/Focus-Perovskites>.
- a) A. M. A. Leguy et al., Chem. Matt. 2015, 27, 3397; b) Y. H. Chang, J. Kor. Phys. Soc. 2004, 44, 889; c) Fang et al., J. Phys. Chem. Lett. 2016, 7, 1596; c) G. Giorgi, K. Yamashita, J. Phys. Chem. Lett., 2016, 7, 888.